Submitted to ApJ

10 June 2002

Dip spectroscopy of the low mass X-ray binary XB 1254−690

A. P. Smale[1], M. J. Church[2,3], and M. Bałucińska-Church[2,3]

ABSTRACT

We observed the low mass X-ray binary XB 1254−690 with the *Rossi X-ray Timing Explorer* in 2001 May and December. During the first observation strong dipping on the 3.9-hr orbital period and a high degree of variability were observed, along with "shoulders" ∼15% deep during extended intervals on each side of the main dips. The first observation also included pronounced flaring activity. The non-dip spectrum obtained using the PCA instrument was well-described by a two-component model consisting of a blackbody with kT=1.30±0.10 keV plus a cut-off power law representation of Comptonized emission with power law photon index 1.10±0.46 and a cut-off energy of $5.9^{+3.0}_{-1.4}$ keV. The intensity decrease in the shoulders of dipping is energy-independent, consistent with electron scattering in the outer ionized regions of the absorber. In deep dipping the depth of dipping reached 100% in the energy band below 5 keV, indicating that all emitting regions were covered by absorber. Intensity-selected dip spectra were well-fit by a model in which the point-like blackbody is rapidly covered, while the extended Comptonized emission is progressively overlapped by the absorber, with the covering fraction rising to 95% in the deepest portion of the dip. The intensity of this component in the dip spectra could be modeled by a combination of electron scattering and photoelectric absorption. Dipping did not occur during the 2001 December observation, but remarkably, both bursting and flaring were observed contemporaneously.

Subject headings: accretion, accretion disks — scattering — (stars:) binaries: close — stars: circumstellar matter — interstellar medium: extinction — stars: individual (XB 1254−690) — X-rays: stars

[1]USRA Research Scientist, Laboratory for High Energy Astrophysics, Code 660.1, NASA/Goddard Space Flight Center, Greenbelt, MD 20771

[2]School of Physics and Astronomy, University of Birmingham, Edgbaston, Birmingham B15 2TT, UK

[3]Astronomical Observatory, Jagiellonian University, ul. Orla 171, 30-244 Cracow, Poland

1. Introduction

Approximately 10% of the low mass X-ray binaries (LMXBs) exhibit X-ray dipping at the orbital period due to absorption in the bulge on the outer accretion disk where the accretion flow from the companion star impacts. Data from these sources provide substantially more information about their system geometry and physics than those from non-dipping sources; physical models for the X-ray emission are strongly constrained by the requirement that they explain not only the persistent non-dip emission spectrum, but also intensity-selected spectra obtained from every level of dipping.

Dips with a recurrence period of 3.88±0.15 hr were discovered in *EXOSAT* data from XB 1254−690 by Courvoisier et al. (1986). Using optical V-band observations of the 19th magnitude counterpart, Motch et al. (1987) determined an orbital ephemeris for dipping of $T_{\rm min}$ = JD 2445735.693 ± 0.004 + 0.163890±0.000009 days, i.e. an orbital period of 3.9334 hr. This ephemeris cannot be extended to the *RXTE* observations described herein because the propogated uncertainty in phase has now become comparable with the orbital period itself. *Ginga* data from XB 1254−690 was used to model spectral evolution in dipping by Uno et al. (1997), in which an "absorbed plus unabsorbed" approach was used, dividing the non-dip spectral form into two components, one absorbed, the other not. However, we can now understand this in terms of spectral effects actually due to the progressive overlap of absorber and extended ADC (see below). In our previous *RXTE* observation of XB 1254−690 on 1997 April 28, dipping activity had apparently ceased (Smale & Wachter 1999). Similarly, dips were not seen in a *BeppoSAX* observation on 1998 Dec 22 (Iaria et al. 2001).

Over the last 10 years it has been shown that one particular physical model has been able to fit the non-dip and dip spectra of all of the other dipping LMXBs. This model consists of point-like blackbody emission from the surface of the neutron star, plus a component due to Comptonized emission from an extended accretion disk corona (ADC) located above the disk (Church & Bałucińska-Church 1985; Church et al. 1997; Smale et al. 2001). Application of this model has revealed details of the emitting regions. In particular, it has been shown that the ADC is very extended, typically 5×10^4 km in radius but varying between 5×10^3 km and 5×10^5 km in different sources (Church 2001), and that the blackbody emission must arise on the neutron star surface rather than in the accretion disk (Church & Bałucińska-Church 2001). In addition, this modeling has allowed the magnitude of the emitting area obtained from observation to be compared (Church, Inogamov, & Bałucińska-Church 2002) with the theory of accretion spreading on the surface of the neutron star of Inogamov & Sunyaev (1999).

It has long been known that spectral evolution in dipping is complex; however application of the above emission model to dip spectra revealed that these changes can be explained

in a straightforward way in terms of an extended absorber progressively overlapping the extended Comptonizing emission region, i.e. the ADC. Thus as dipping progresses, a fraction of the ADC is covered by absorber, giving a strongly absorbed component of the spectrum, while the remaining part is unabsorbed. The neutron star blackbody emission, by contrast, is covered almost instantaneously, suffering rapidly increasing column density. This progressive covering model has been shown to explain dipping in the sources XB 1916−053 (Church et al. 1997), in XBT 0748−676 (Church et al. 1998), in XB 1323−619 (Bałucińska-Church et al. 1999) and in X 1624−490 (Bałucińska-Church et al. 2000; Smale et al. 2001). In the case of X 1624−490, the so-called Big Dipper, an additional feature has been observed that was not previously detected in other dipping LMXBs, that of shoulders of dipping (Smale et al. 2001). The light curve for X 1624−490 clearly reveals two stages of dipping: first, a decrease in intensity of about 15% lasting 12,000 s; next, the onset of deep dipping with rapid variability showing removal of the point-source emission, lasting 20,000 s. Spectral investigation of the shoulders of dipping revealed that there was no increase of column density for a shoulder spectrum selected in an appropriate intensity band. The spectrum could, however, be modeled by assuming that electron scattering produced an energy-independent decrease of intensity. This suggests a physical picture in which the bright X-ray emission from the central source results in complete ionization of the outer layers of absorber, giving rise to shoulders of dipping as soon as the ADC is overlapped by absorber. Regions deeper inside the absorber are not fully ionized, and increases in column density are detected as the neutron star is overlapped.

In the present work we show that XB 1254−690 has marked similarities with X 1624−490. It has shoulders of dipping, and strong variability in deep dipping. Moreover, it exhibits strong X-ray flares at higher energies, the physics of which has thus far been poorly understood. Our analysis of flaring in X 1624−490 (Bałucińska-Church et al. 2001) has discussed the physical changes occurring at the inner disk and neutron star. In this paper, we present results of investigating spectral evolution during dipping in XB 1254−690. A follow-up paper (Church, Bałucińska-Church, & Smale 2002; Paper II) will contain a full analysis of the flaring observed in this source.

2. Observations

XB 1254−690 was observed using the *Rossi X-ray Timing Explorer (RXTE)* (Bradt, Rothschild, & Swank 1993) on two occasions in 2001: from May 9/23:26–May 12/11:55 UT, covering 15.4 binary cycles of the 3.9334-hr orbital period, with a total on-source good time of 64.7 ksec, and from Dec 6/11:04 – Dec 7/14:46, covering 7.0 binary cycles with

a total of 64.9 ksec of on-source good time. The data presented here were collected by the proportional counter array (PCA) instrument using the Standard 2 and Good Xenon configurations, with time resolutions of 16 s and 0.95 μs respectively. The PCA consists of five Xe proportional counter units (PCUs) numbered 0–4, with a combined total effective area of about 6500 cm^2 (Jahoda et al. 1996). PCUs 0, 2, and 3 were reliably on during the first observation, and PCUs 0 and 2 during the second. However, the observations presented here occurred subsequent to the loss of the propane layer in PCU0. The loss of this window has led to a higher background countrate in this detector, and also in a gain difference for PCU0 such that at 20 keV the channel-energy relationship for PCU0 differs from the other PCUs by >1 keV. For these reasons we chose to exclude data from PCU0 when performing the detailed spectral fitting work described below.

The PCA light curves and spectra were extracted using the standard *RXTE* analysis software, FTOOLS 5.1, and spectral fitting was performed using XSPEC. As the persistent emission count rate per PCU was greater than 40 c s^{-1}, background subtraction was first attempted using the epoch 4 "bright" model recommended for epoch 5 (*skyvle_e4v20000131*, *allskyactiv_e4v20000131*). However, comparison of the background and source spectra at energies >30 keV (where the source does not contribute significantly) showed that the generated background was not a good fit to the source spectrum, exceeding the source spectrum by $\sim$ 10%. Next we tried the "faint" model (*l7_e4v19991214*, *240_e4v19991214*) and found that it gave an excellent matching of the background and source spectra at energies of 30–100 keV. Therefore, we adopted this model for background subtraction. While this analysis was in progress newer versions of the PCA background models became available, but experimentation showed that adopting the new models made a negligible difference to the parameters we derived from our spectral fits. Deadtime corrections were applied to all source spectra, and systematic errors of 1% added to the fits. The light curves have been barycentrically corrected.

Data were also obtained using the HEXTE phoswich detectors, which are sensitive over the energy range 15–200 keV. The source was detected in both observations with a background-subtracted count rate of $\sim$2 c s^{-1}, with the bulk of these counts in the 15–30 keV range. Deadtime-corrected HEXTE spectra and light curves were obtained using the *hxtlcurv* tool with 16 s time binning, but it was discovered that adding the HEXTE data to the spectral fits did not appreciably improve the fitting or the accuracy of determining spectral parameters.

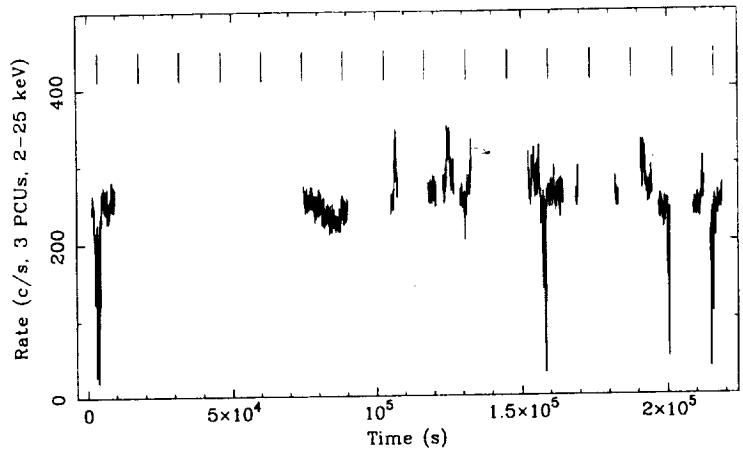

Fig. 1.— The *RXTE* PCA light curve of XB 1254−690 obtained on 2001 May 9–12 shows strong dipping and flaring. The vertical ticks are separated by the orbital period of 3.9334 hr and indicate the expected times of dips. The dip expected at $\sim 8.87 \times 10^4$ s is not seen. The binsize is 32 s.

3. Results

3.1. X-ray light curves

Figure 1 shows the light curves for the two observations, derived from PCA Standard 2 data in the 2–25 keV band. The first observation shows evidence for deep dipping. We obtained complete coverage of the first dip, and combining the time of dip center with the accurate orbital period derived by Motch et al. (1987), we noted that 16 dipping intervals fall within the observation. Of these, the data cover only 7, the rest being lost to Earth occultation, SAA passage, and observations of other sources. Two full dips are observed, one at the beginning of the observation, and the other centered 1.59×10^5 s into the observation. This later dip did not reach 100% depth and is possibly contaminated by flaring. Partial dips are observed at 1.31×10^5 s, 2.02×10^5 s, and 2.16×10^5 s. The dip predicted at 8.87×10^4 s apparently did not occur.

In the second observation the *RXTE* coverage is more continuous (Figure 2). Seven consecutive dips are predicted, but no periodic flux reductions are evident. The data contain three Type I bursts, two of them falling close to the predicted time of X-ray dips.

Both observations contain significant flaring episodes. We extracted and examined light curves in various energy bands within the PCA range, and discovered that the flaring is limited to the data above 7 keV; in this, XB 1254−690 strongly resembles X 1624−490

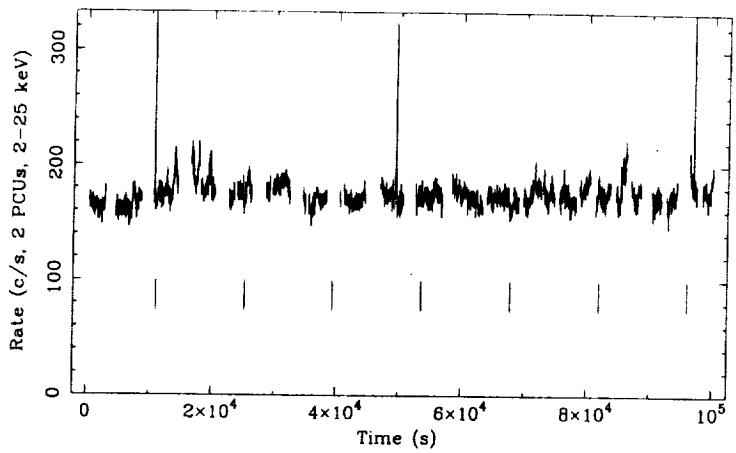

Fig. 2.— The light curve from 2001 Dec 6–7, showing three bursts and sporadic flaring. Again, the vertical ticks indicate the expected times of dips, as extrapolated from the earlier observation using the period derived by Motch et al. (1987).

(Bałucinska-Church et al. 2001). A complete analysis of physical changes taking place during flaring in XB 1254−690 will be presented in an upcoming paper (Church et al. 2002a).

Figure 3 shows a light curve of the dip early in the first observation in four energy bands: 2–5 keV, 5–10 keV, 10–25 keV, and the total range 2–25 keV, using Good Xenon data with 1s time bins. This figure shows that the dipping remarkably reaches 100% in all energy bands. Such behavior is also seen up to 10 keV in the dipping source X 1916−053, showing that the absorber has larger angular extent than all emission regions (Church et al. 1997). In Figure 3 we also see that XB 1254−690 exhibits clear "shoulders" of dipping, i.e. regions both before and after the deep dipping in which there is a small decrease of intensity. Each shoulder of the dip lasts ∼650–925 s, during which the total count rate in the 2–25 keV band drops by ∼15%. The shoulder is followed by an interval of strongly variable deep dipping lasting ∼1100 s. Taking this into account, a full dip lasts ∼3000 s, equivalent to ∼21% of the orbital cycle.

This behavior has also been seen in X 1624−490, which has marked shoulders of dipping lasting 10 20 ks each side of the main dipping, first seen in *EXOSAT* data (Frank, King & Raine 1992; Church & Bałucińska-Church 1995). In our analysis of *RXTE* data from X 1624−490 we found that the shoulders are almost certainly due to electron scattering in the outer fully ionized layers of the absorber (Smale et al. 2001).

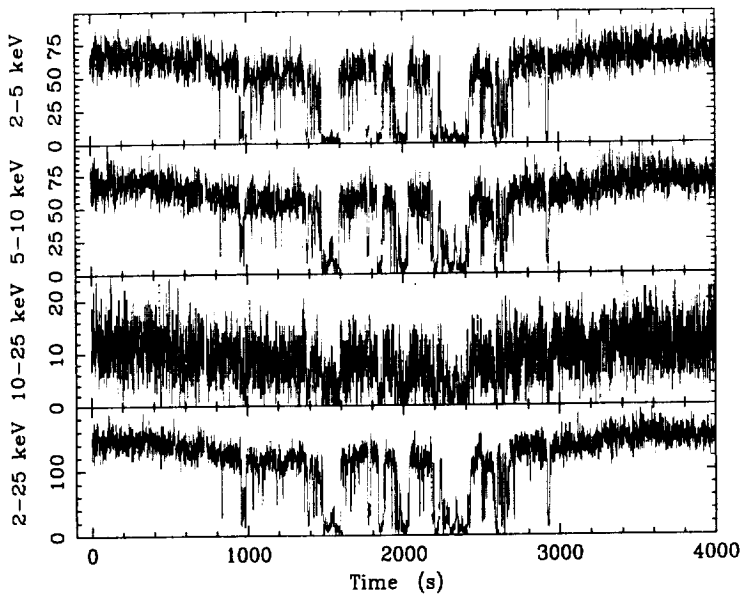

Fig. 3.— Expanded light curve for the first dip used for spectral analysis showing 100% deep dipping, the rapid variability in several sub-bands, and the total band 2–25 keV.

3.2. Hardness ratios

In Figure 4 we compare the variation of hardness with overall intensity in X 1254−690 with that of X 1624−490 (Smale et al. 2001). Here, the hardness ratio is defined as the ratio of the counts in the 10–25 keV and 2–5 keV bands. This representation shows that there are strong similarities in the behavior of the two sources.

First, the increase of hardness during X-ray flaring can be seen in both sources. Experimentation shows that this flaring is predominantly a higher energy phenomenon seen above ∼7 keV in the light curves, leading to the hardness increase. Immediately below the non-dip level in XB 1254−690 (marked on Fig. 4) are the shoulders of dipping seen in the light curve. Neither source shows a change in hardness ratio between non-dip and the shoulders of dipping. Finally, in deeper dipping there are strong changes in hardness ratio, first an increase of hardness and then a strong softening in the deepest portion of the dip. Studies of X 1624−490 (Church & Bałucińska-Church, 1995; Smale et al. 2001) have shown that the softening in deepest dipping in that source was due to complete removal of the rather hard neutron star blackbody from the spectrum.

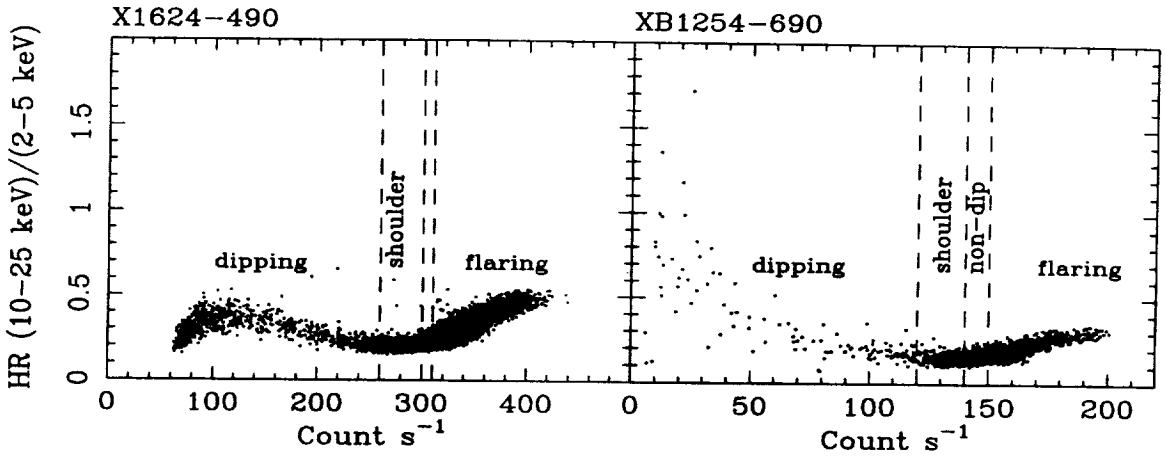

Fig. 4.— Hardness as a function of intensity for the *RXTE* observation of X 1624−490 in 2000 (left panel) and for the present observation of XB 1254−690 (right panel). The intensity bands where flaring, dipping and persistent emission predominate are marked with vertical lines (see text).

3.3. Persistent emission spectrum

We confine our spectral analysis to the high quality data of the first dip (Fig. 3), as this appeared to be entirely free from X-ray flaring which would strongly modify the spectra, the dip was very deep and not broken by data gaps, and because there were small overal changes in non-dip intensity with time which make it undesirable to select data in intensity bands across the whole observation. Figure 3 shows that dipping is essentially 100% deep in the lowest energy band of 2–5 keV which implies that the absorbing region has larger angular extent than all source regions.

As rapid variability took place during the dipping, selection of the persistent and dip spectra was made using the PCA data obtained with high time resolution in Good Xenon mode. The persistent spectrum was selected using good time intervals based on the 1 s light curve in the 2–25 keV band, using the top layers of PCU 2 and PCU 3 in the 140–150 c s^{-1} intensity band. Spectral fitting was done with the two-component model described in the Introduction, consisting of a point-like blackbody emission component associated with the neutron star, plus Comptonized emission from a very extended accretion disk corona (ADC) (Church 2001), represented using a cut-off power law with interstellar absorption:

$$\mathrm{AG}^*(\mathrm{BB} + \mathrm{CPL})$$

As the lowest well-calibrated energy in PCA data is ~2.5 keV, it is not possible to accurately

constrain column density from spectral fitting. In our spectral fitting we thus froze the Galactic column density at the value measured towards XB 1254−690 in the 21 cm radio survey of Dickey and Lockman (1990): 0.29×10^{22} cm^{-2}. We present the fit to the persistent emission in Figure 5, and the fit parameters in Table 1; errors quoted are 90% confidence.

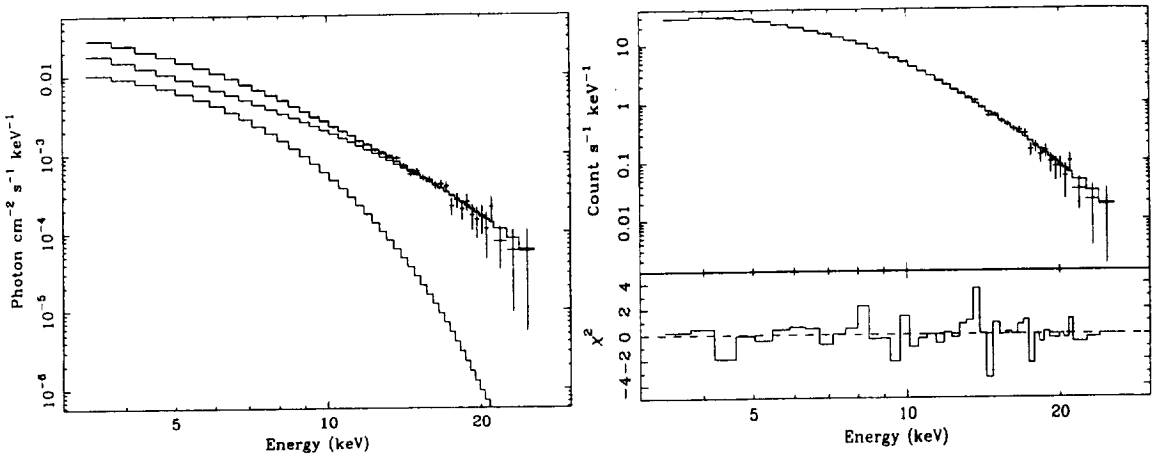

Fig. 5.— Spectrum of the non-dip emission. Left: the total model, blackbody and cut-off power law components, and data. Right: the folded spectrum.

3.4. Spectral evolution during dipping

Dip spectra were selected from the first dip in seven intensity levels to cover the shoulders of dipping, intermediate dipping, and deep dipping. The analysis was carried out for spectra selected in two different ways. First, spectra were selected in intensity bands across the whole dip. However, Fig. 3 shows the high degree of variability during dipping, implying that it may be difficult to avoid mixing data from different intensity bands in the selection. This was the reason that the intensity selection was made using a light curve with 1-second binning. To test this possibility, a second data selection was performed using a subset of data selected between times 2200–2400 s in Fig. 3, to include only data from a sub-dip during which there were no excursions back to non-dip intensity. In this way possible effects due to mixing data due to the rapid variability were avoided. Although the count statistics for the second set of spectra were degraded compared with spectra obtained from the whole dip, the results clearly agreed with those of the first set, from the whole dip, and showed no evidence for mixing effects (which may, for example, be manifested as difficulty in fitting intermediate-level dip spectra). Hence we proceeded using spectra obtained from data from the whole dip.

First, the two-component progressive covering model was applied to these spectra:

$$\mathrm{AG}^{*}(\mathrm{AB}_1 * \mathrm{BB} + ((1 - f) + \mathrm{AB}_2 * f) * \mathrm{CPL})$$

where AB_1 and AB_2 are the additional absorption of the blackbody and cut-off power law components respectively, and f is the covering factor of the cut-off power law component. Fitting was carried out with the emission parameters frozen (kT_{BB}, Γ etc.), as these do not change during dipping. In shallow dipping, the blackbody component required little additional column density; in deep dipping, the column density was very high as expected. However, when applied to the dip shoulder spectrum this model required an artificially-large value of N_{H} for the cut-off power law component. The shoulder spectrum had a slightly decreased intensity at all energies compared with the non-dip spectrum, and fixing the emission parameters (including the normalization) at non-dip values resulted in this energy-independent decrease being spuriously modeled by a large increase in column density, when in reality the spectrum showed no evidence for a genuine increase of N_{H}. The energy-independent, vertical shift downwards of the shoulder spectrum implies that electron scattering in the outer highly-ionized regions of the accretion disk was taking place, as in X 1624−490 (Smale et al. 2001). Consequently, we replaced the progressive covering term applied to the cut-off power law with the following model:

$$f\, e^{-N_e \sigma_T}\, e^{-N_H \sigma_{PE}} + (1 - f)$$

such that an electron scattering term described by an electron column density N_e and the Thomson cross section σ_T is added to the photoelectric absorption in the progressive covering term.

Using this model, sensible fit results were obtained for the shoulders of dipping and for deeper levels of dipping. Spectral fits were performed keeping the best-fit parameters of the persistent emission frozen at the values shown in Table 1. The folded and unfolded spectra with fits are shown in Figure 6, and the best-fitting parameters for the shoulder and dip spectra are given in Table 2. In Figure 7 we show the evolution of the column densities and covering fraction with count rate during the dipping.

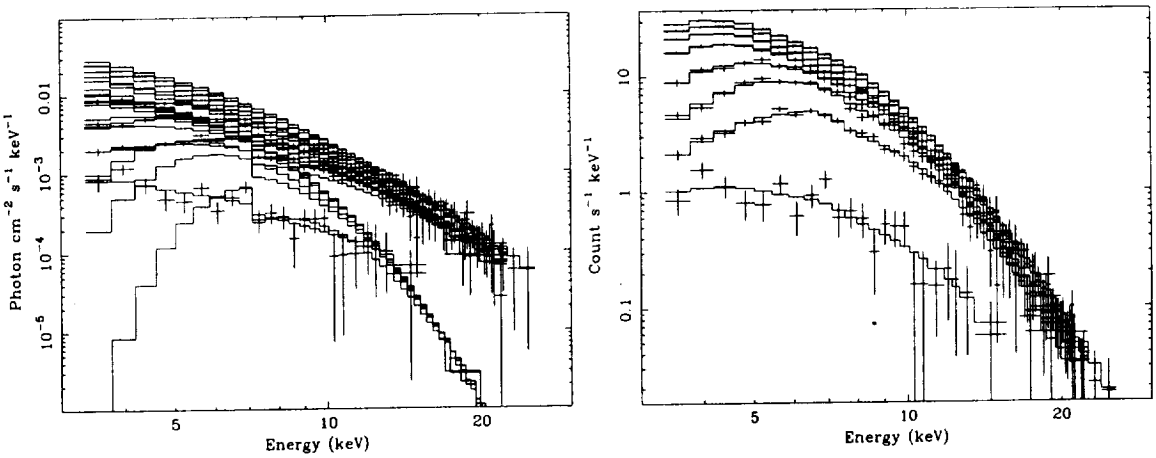

Fig. 6.— Spectral fitting of the dip spectra. Left: the unfolded spectra with the total model and data. Right: the folded spectra.

4. Discussion

The extended *RXTE* observation of XB 1254−690 of 2001 May 9–12 reveals very deep X-ray dipping, as well as strong X-ray flaring. The second observation, performed on 2001 Dec 6–7, remarkably exhibits both X-ray flaring and X-ray bursts – but no dipping – and will be discussed in Paper II. The high degree of variability during dipping on relatively rapid timescales is associated with absorption of point-source emission, and demonstrates the blobby nature of the absorber. In addition to this rapid variability, we also detected for the first time in this source extended shoulders of dipping both before and after the deep dipping. Similar shoulders are seen in X 1624−490 (Frank et al. 1992; Church & Bałucińska-Church 1995), and our previous work shows that the shoulders are almost certainly caused by electron scattering in the outer layers of the absorber (Smale et al. 2001). In XB 1254−690 these shoulders of dipping consist of a 15% decrease in intensity lasting ∼650–925 s on either side of deep dipping which lasts ∼1100 s. The shoulders coincide with the envelope defining the total time that source regions are overlapped by absorber, and the total dip ingress time consists of the shoulder duration plus the transition to deep dipping. The length of the envelope clearly demonstrates the very extended nature of one of the emission components in the source, and, together with the dip ingress time, will be discussed below.

We carried out spectral fitting of the non-dip emission and of 7 dip levels. Simple models were unable to fit the complex spectral changes. However, good fits were obtained by using a combination of a two-component emission model with a progressive covering absorption model. This emission model has previously been shown to fit the other dipping

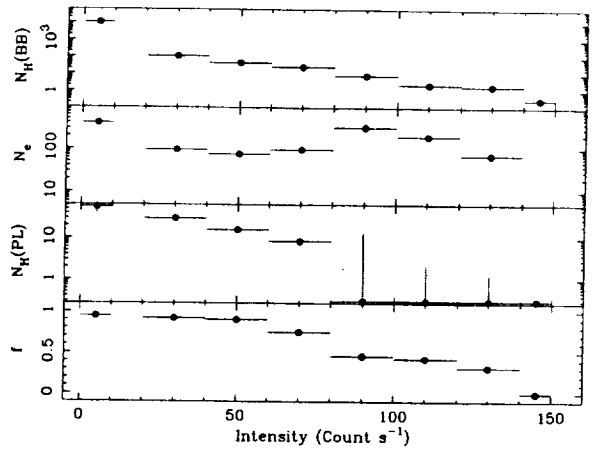

Fig. 7.— Evolution of column densities and covering fraction from non-dip values during dipping. The electron column density cannot be shown for the non-dip spectrum as the value is zero.

sources, i.e. XB 1916−053 (Church et al. 1997), XBT 0748−676 (Church et al. 1998), XB 1323−619 (Bałucińksa-Church et al. 2001) and X 1624−490 (Church & Bałucińska-Church 1995; Smale et al. 2001), and consists of point-like blackbody emission from the surface of the neutron star, plus Comptonized emission from an extended ADC. The spectral evolution during dipping in all these sources reveals a part of the spectrum which is unabsorbed plus part which is strongly absorbed, well-modeled by progressive covering in which the spatially extended absorber progressively overlaps the extended Comptonizing ADC. In XB 1254−690 the progressive approach also fits well giving further confidence that the combination of the two-component emission model with progressive covering is the correct description of these sources. We find that the non-dip spectrum is well-described by a simple blackbody of kT = 1.30±0.10 keV, and a cut-off power law description of Comptonization with power law index Γ = 1.10±0.46 and cut-off energy $5.9^{+3.0}_{-1.4}$ keV, combined with a (fixed) column density of 0.29×10^{22} cm^{-2}. During dipping the covering fraction f rises from zero to ∼95%.

In both XB 1254−690 and X 1624−490 (Smale et al. 2001), we have discovered extended shoulders of dipping. The spectra of the shoulders show no evidence for increased column density relative to the non-dip spectrum, but only for an energy-independent decrease of intensity. We have shown that the shoulders are well-fitted by adding an electron scattering term to the normal absorption term required for deep dipping. In XB 1254−690, there is some possible competition between N_H and electron column density N_e, but N_e increases to a high value in the early stages of dipping, as would be expected in terms of the outer layers of absorber being highly ionized by the central source so that N_H is small, but N_e large.

The most important consequence of progressive covering is that it proves by itself that the Comptonizing region producing the hard, non-thermal emission must be very extended if it is only gradually overlapped by absorber. The long dip ingress time confirms this, as seen by the long period over which intensity decreases in the shoulders of dipping (Fig. 3), which is then continued as dipping deepens. In other dipping sources, dip ingress measurements have also revealed a very large size for the radius r_{ADC} of the Comptonizing ADC; typically 50,000 km, but varying between 5,000 and 500,000 km for different sources (Church, 2001). The fact that the depth of dipping reached 100% in this source confirms that the envelope of the absorber has larger angular extent than the most extended emission region, i.e. the ADC. In this case, the ingress time Δt depends on the source diameter, and

$$2\,\pi\,r_{disk}/P = d_{ADC}/\Delta t$$

where r_{disk} is the disk radius, P is the orbital period, and d_{ADC} is the diameter of the ADC, since the ingress times depend on the velocity of material in the outer disk. In addition, the total duration of dipping, i.e. between times when the intensity is at the non-dip level, depends on the sum of the extended source diameter and the absorber diameter, which we will also use below. Because of the strong variability during dipping in XB 1254−690 it is less easy to determine an accurate dip ingress time than in sources where there is no variability. However, the total duration of dipping is well-determined at 3000±100 s, as is the duration of deep dipping at 1100±100 s (measured from when the depth of dipping first reaches reaches 100% till it last reaches 100%). From these we obtain a dip ingress time Δt of 950±140 s. Using an orbital period of 14.16 ksec (=3.93 hr) and a neutron star mass of 1.4 $M_{\odot}$, an accretion disk radius can be calculated of 4.08×10^{10} cm (Frank et al. 1987). From the value of Δt, we then derive a value of r_{ADC} of $1.77 \pm 0.14 \times 10^{10}$ cm, i.e. 177,000±14,000 km. This value again demonstrates the very extended nature of the ADC, which has fundamental consequences for the understanding and theoretical modeling of LMXBs.

Previously, theoreticians have commonly presented a picture of LMXBs in which Comptonization takes place in a small region centered on the neutron star. This approach was considered natural in view of the expectation that regions of hot electrons might reasonably be expected to be located close to the neutron star, and might well have spherical symmetry. Examples of this theoretical approach include Kluzniak & Wilson (1991), Barret et al. (2000), Popham & Sunyaev (2001), and Done, Zycki & Smith (2002). However, the measurements of dip ingress times rule out the possibility of such a small central Comptonizing region. An ADC radius of 50,000 km is 1000 times larger than expected for a small central region. The progressive covering observed in dipping also demonstrates that one emission region is very extended, by the very gradual removal of this component. It must therefore

be concluded that theoretical approaches based on a small central Comptonizing region are not correct.

This, of course, refers to the major Comptonized emission component that dominates the spectra of low mass X-ray binaries in their usual state of persistent emission. It does not rule out possible modification of the other emission component, the neutron star blackbody emission that has been inferred to take place in some X-ray bursts, nor does it apply to transiently-accreting neutron stars in quiescence (at luminosities of 10^{33} erg s^{-1}), when the neutron star blackbody emission is expected to be modified by percolation of high energy photons upwards in the atmosphere (Rutledge et al. 2000). The extent to which modification of the blackbody emission takes place in bursts, flares and non-burst emission is discussed by Bałucińska-Church et al. (2001).

REFERENCES

Bałucińska-Church, M., Barnard, R., Church, M. J. & Smale, A. P. 2001, A&A, 378, 847

Bałucińska-Church M., Church M. J., Oosterbroek T., et al., 1999, A&A, 349, 495

Bałucińska-Church M., Humphrey P. J., Church M. J., & Parmar A. N., 2000, A&A, 360, 583

Barret, D., Olive, J. F., Boirin, L., Done, C., Skinner, G. K., & Grindlay, J. E. 2000, ApJ, 533, 329

Bradt, H. V., Rothschild, R. E., & Swank, J. H. 1993, A&AS, 97, 355

Church, M. J. 2001, AdSpR, 28, 323

Church M. J., & Bałucińska-Church M., 2001, A&A, 369, 915

Church, M. J., & Bałucińska-Church, M. 1995, A&A, 300, 441

Church M. J., Bałucińska-Church M., Dotani T., & Asai K. 1998, ApJ, 504, 516

Church, M. J., Bałucińska-Church, M., & Smale, A. P. 2002, A&A, in preparation (Paper II)

Church, M. J., Dotani, T., Bałucińska-Church, M., Mitsuda, K., Takahashi, T., Inoue, H., & Yoshida, K. 1997, ApJ, 491, 388

Church M. J., Inogamov N. A., & Bałucińska-Church, M. 2002, A&A, in press

Courvoisier, T. J.-L., Parmar, A. N., Peacock, A., & Pakull, M. 1986, ApJ, 309, 265

Dickey, J. M., & Lockman, F. J. 1990, ARA&A, 28, 215

Done, C., Zycki, P. T., Smith, D. A. 2002, MNRAS, 331, 453

Frank, J., King, A., & Raine, D. 1992, Accretion Power in Astrophysics. 2nd ed., Cambridge, UK: Cambridge University Press.

Iaria, R., Di Salvo, T., Burderi, L., & Rossa, N. R. 2001, ApJ, 548, 883.

Inogamov N. A., & Sunyaev R. A., 1999, Astron Lett 25, 269

Jahoda, K., Swank, J. H., Giles, A. B., Stark, M. J., Strohmayer, T., Zhang, W., & Morgan, E. H. 1996, in EUV, X-ray and Gamma-Ray Instrumentation for Astronomy VII, ed O. H. Siegmund (Bellingham, WA: SPIE), 59

Kluzniak, W., & Wilson, J. R. 1991, ApJ, 372, L87

Motch, C., Pedersen, H., Beuermann, K., Pakull, M. W., & Courvoisier, T. J.-L. 1987, ApJ, 313, 792

Popham, R., & Sunyaev, R. A. 2001, ApJ, 547, 355

Rutledge, R. E., Bildsten, L., Brown, E. F., Pavlov, G. G. & Zavlin, V. E. 2000, ApJ, 529, 985

Smale, A. P., Church, M. J., & Bałucińska-Church, M. 2001, ApJ, 550, 962

Smale, A. P., & Wachter, S. 1999, ApJ. 527, 341

Uno S., Mitsuda K., Aoki T., & Makino F, 1997, PASJ, 49, 353

Table 1. Results of fit to PCA persistent (non-dip) emission spectrum.

N_H 10^{22} cm^{-2} (Frozen)	kT_{BB} keV	I_{BB} 10^{36} erg s^{-1} @10 kpc	Γ	E_{CO} keV	I_{PL} ph s^{-1} cm^{-2} keV^{-1}	χ^2/d.o.f.
0.29	$1.30^{+0.10}_{-0.12}$	$4.3^{+0.8}_{-0.9}$	1.10 ± 0.46	$5.9^{+3.0}_{-1.4}$	$0.14^{+0.06}_{-0.05} \times 10^{-2}$	32.6 / 40

Table 2. Best fits to the shoulder and dip spectra

	N_H(BB) 10^{22} cm^{-2}	N_H(CPL) 10^{22} cm^{-2}	f_{cov}	N_e 10^{22} cm^{-2}	χ^2/d.o.f.
shoulder: 120 – 140 c s^{-1}	1.8 ± 0.4	$0.3^{+1.0}_{-0}$	0.313 ± 0.022	70 ± 7	35.8/38
shoulder: 100 – 120 c s^{-1}	2.3 ± 0.5	$0.3^{+1.9}_{-0}$	0.425 ± 0.014	194 ± 13	42.2/35
dip: 80 – 100 c s^{-1}	7.8 ± 1.6	0.3^{+13}_{-0}	0.456 ± 0.028	315^{+90}_{-60}	18.0/29
dip: 60 – 80 c s^{-1}	25 ± 3	$8.4^{+2.1}_{-1.4}$	0.748 ± 0.036	95 ± 12	23.1/29
dip: 40 – 60 c s^{-1}	43^{+5}_{-4}	$15.9^{+1.5}_{-0.6}$	0.899 ± 0.020	75^{+8}_{-5}	25.6/31
dip: 20 – 40 c s^{-1}	104^{+12}_{-9}	30 ± 2	0.916 ± 0.010	94 ± 7	25.3/30
dip: 0 – 10 c s^{-1}	$> 10^4$	57^{+32}_{-18}	0.945 ± 0.007	390 ± 60	19.5/19